

2. Palmer Station (06/01/23 – 05/31/24)

This sections describes quality control of solar data recorded at Palmer Station between 06/01/23 and 05/31/24. The period resulted in a total of 17,440 solar scans, which were assigned to Volume 33. There was no site visit during the reporting area.

Solar data of the reporting period were affected by multiple issues:

- Instability in the responsivity of the SUV-100 spectroradiometer due to punctured diffuser
 The Research Associate at Palmer Station reported on 1/2/24 that the diffuser of the SUV-100 spectroradiometer was punctured, most likely by a Snowy Sheathbill pecking on it. However, data analysis indicated that the diffuser may have already been compromised by as early as October 2023. There was no spare diffuser on site. A replacement was manufactured by Biospherical Instruments, Inc and was installed on 4/9/24. (Note that a similar issue also occurred during the previous reporting period.) As a result of the puncture, water was able to get into the instrument’s collector, which caused changes in the responsivity of the system between mid-October 2023 and until the diffuser’s replacement. Changes in responsivity were assessed by comparing data from the SUV-100 with measurements of the collocated GUV-511 radiometer and radiative transfer modeling. These comparisons showed that changes in responsivity ranged in the order of $\pm 10\%$ with little dependence on wavelength. Most SUV-100 data could be corrected for these fluctuations with the help of GUV-511 data. (This correction assumed that the GUV-511 instrument was stable during the reporting period, which is a good assumption based on past records of the instrument.) SUV-100 data that were collected during times when measurements of the SUV-100 and GUV-511 systems could not be brought into agreement were not published. The rejection criterion was conservative and may have also removed data from periods when measurements were affected by other causes such as the accumulation of snow on the collectors of the SUV-100 or GUV-511. A summary of missing data is provided in Section 2.4.
- Uncertainty of the cosine error correction
 Data analysis further revealed that the cosine error of the instrument’s collector was different from that of past seasons. This was to be expected because a new diffuser was installed during the previous reporting period and because of the effect of the puncture in that new diffuser. A new cosine error correction was therefore established. This was challenging and is subject to uncertainties due the effect of the puncture on the instrument’s stability and the lack of a sufficient number of clear sky scans, which form the basis of the parameterization. The new correction function is based on about 200 scans recorded during clear skies between 10/28/23 and 1/22/24. The new function corrects the cosine error affecting scans measured during this period well. However, the new function tends to overcorrect clear sky scans measured between July and September 2023 and during April 2024. About 150 scans are affected and were flagged in the Version 2 dataset. Scans measured during overcast conditions (which is the norm at Palmer Station) are not affected. Those scans were scaled up by the standard diffuse correction factor of 1/0.95, as it was the case in past seasons. The uncertainty of spectra measured under cloudy conditions is therefore comparable to that of measurements in the past. Hence, the issue affects less than 1% of all scans recorded.
- Instability of internal lamp
 The brightness of the internal lamp decreased by about 1% over the reporting period, which is within the normal range. However, there were also 20 scans of that lamp during which the lamp did not burn stable. These scans were not used for the processing of solar data and this issue therefore does not affect the quality of published data. However, since the reason for these instabilities could not be identified, there is the risk that data of the next reporting period might be affected if the problem worsens.

- Failure of the 320 nm channel of the GUV-511 radiometer
 The 320 nm channel of the system's GUV-511 became defective in the later half of 2022, resulting in a large non-linearity. As it was the case during the previous reporting period, solar data of the GUV-511 radiometer had to be produced without using the 320 nm channel. Thus, UV data products are based on measurements of the 305, 340, and 380 nm channels only. Comparisons with data from the SUV-100 spectroradiometer performed during the previous reporting period confirmed that the quality of minute-by-minute data in "GUV2" files is still adequate. However, "GUV1" data that are coinciding with SUV-100 measurements showed large fluctuations during cloudy conditions. Data products that rely on measurements of all three channels (specifically data labeled "Dose1", "Dose2", "CIE", "UVIndex", "Erythema_Anders", "RBM501", "SCUP-h", "SCUP-m", "Flint", "Boucher", "Cullen_phaerodactylum", "Cullen_prorocentrum", and "Neale_Antarctic") were removed from the "GUV1" files. Data products that are based on measurements of only two channels are less impacted and were included in the data files but are also less accurate than historically. It can be concluded that "GUV2" data can be used, for example, to fill in gaps in SUV-100 data, but **"GUV1" data should not be used.**
- Time errors
 The system's time was historically synchronized with the help of a GPS receiver. The device failed on 6/16/22 and cannot be repaired. Since this time, the system time is adjusted manually. During the reporting period, the system time was advanced by ">30 seconds" on 8/7/23, by about one minute on 9/8/23, by about three minutes on 1/7/24, and by about two minutes on 5/22/24. Data were not corrected for these drifts in time. It is planned for the future to synchronize time via an Internet time server. Of note, since the SUV-100 and GUV-511 radiometers are controlled by the same computer, the two data streams remain synchronized relative to each other.

The system's PSP radiometer was unit 30450F3 and has a calibration factor of $8.885 \times 10^{-6} \text{ V}/(\text{W m}^{-2})$, which was established on 11/1/17. TUVR data were erratic and were not published.

2.1. Irradiance Calibration

On-site standards

The on-site irradiance standards for the reporting period were the lamps 200W007, M700, M765, 200WN009, and 200WN010. Lamps 200WN009, and 200WN010 are "long-term" standards, which were left at Palmer Station during the March 2014 site visit. It was the original intent to run lamp 200WN009 once per year to compare with the other on-site standards and to run 200WN010 every other year during site visits when all on-site lamps and the traveling standard are compared with each other. Both long-term standards were used once during the reporting period.

Long-term standards

The long-term standards 200WN009 and 200WN010 were calibrated on 12/20/2013 against lamps 200WN001 and 200WN002; see previous Operations Reports for details.

Working standards

The working standards M700 and M765 were recalibrated during the preparation of Volume 28. The scales of irradiance of these two working standard used for the processing of Volume 33 data are identical to those applied to Volumes 28–32. The working standard 200W007 was recalibrated against the average scale of working standards M700 and M765 using absolute scans executed on 7/1/23.

Adjustment of calibration scale

In early 2020, the chain of calibrations applied between 1996 and 2019 to solar data of the NSF and NOAA monitoring networks was re-evaluated (Bernhard and Stierle, 2020). This analysis suggested that the scale of spectral irradiance of NIST standard F-616, which has been used as the primary standard since 2013, is low compared to the scale of primary standards used before 2013. This bias is -2% at 300 nm, -1% at 375 nm, and less than $\pm 0.5\%$ between 420 and 600 nm. **Version 2 solar data of Volume 33 were**

scaled upward accordingly; however, Version 0 remain traceable to the original scale of the primary standard F-616.

Comparison of calibration lamps

Figure 1 shows a comparison of the scales of spectral irradiance of all lamps used during the reporting period relative to the average scale of all lamps, excluding the long-term standard 200WN010. The plot is based on absolute scans performed on 10/2/23. The scales of lamps M765, 200W007, M700, and 200WN009 agree to within $\pm 1\%$ in the UV and 0.5% in the visible range. However, the scale of the long-term standard 200WN010 is higher by 1.0% on average for the wavelength range 290–600 nm. A similar bias was also observed in the past. This indicates that the scales of the two lamps has not drifted; instead, there is a small difference, which has always existed and which is within the uncertainty of the lamp’s calibrations. (If the scale of lamp 200WN010 were the correct scale and solar data had been calibrated against this scale, they would be larger by about 1.0% on average.)

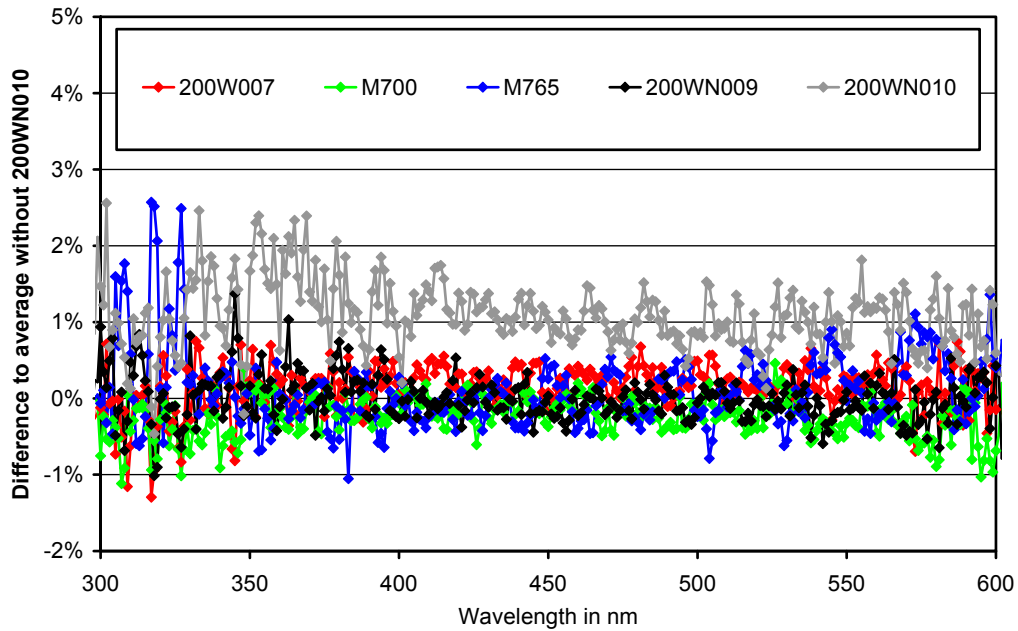


Figure 1. Comparison of the calibration of on-site and long-term standards on 10/02/23.

To further validate the irradiance scale of solar measurements of the SUV-100 spectroradiometer, the GUV-511 radiometer was vicariously calibrated against the subset of SUV-100 measurements that was not affected by the instrument’s instability described above. Calibration factors calculated with this method were compared with similar factors established during previous years. The analysis showed that calibration factors for the GUV-511’s 305, 340, and 380 channels were larger by 2.4%, 1.5%, and 0.5%, respectively, compared to the average of similar factors established for data of the 2015/16 (Volume 25) through 2021/22 (Volume 31) periods. (Data from the 2022/23 (Volume 32) were not included in the average because of the uncertainty stemming from the punctured diffuser during that period; see the report of the previous reporting period.) This result confirms the good consistency of SUV-100 calibrations over extended periods of time.

2.2. Instrument Stability

The short-term radiometric stability of the SUV-100 spectroradiometer was monitored with calibrations utilizing the on-site irradiance standards, with daily “response” scans of the internal lamp, by comparison with measurements of the collocated GUV-511 multifilter radiometer, and by comparisons with results of a radiative transfer model (part of “Version 2” data, see Bernhard et al. (2004)).

Figure 2 shows results from measurements of the internal lamp. Specifically, readings of the instrument’s TSI sensor (a filtered photo diode with sensitivity mostly in the UV-A) are compared with measurements of the SUV-100’s PMT at 300 and 400 nm, derived from response scans performed between 6/1/23 and 5/31/24. TSI measurements decreased by about 1% during this period, indicating that the internal lamp became dimmer by this amount. (Fluctuation at the 0.5% level in the TSI measurements are the result of the resolution of the digitally-controlled 12-bit power supply that powers the lamp.) However, there were also 20 scans during the reporting period, mostly between 9/8/23 and 9/21/23 and between 11/7/23 and 11/27/23, where the internal lamp did not burn stable. Several of these scans are indicated in Figure 2. (Ratios for several scans are off scale.) Affected scans were not used for processing of solar data. PMT currents at 300 and 400 nm increased abruptly by 2% on 8/16/23 for unknown reasons, decreased by about 2% over the following months, and increased again by 2% on 4/10/24 after the replacement of the diffuser. (The increase was not expected because the diffuser is not in the light path of the internal lamp. The actual reason for the increase is therefore unknown). While still small, the fluctuations of PMT currents are larger than the variation in the TSI signal, suggesting variations in either the monochromator’s throughput or the PMT’s sensitivity. By “pairing” solar scans of a particular day with the response scan of that day, most of these fluctuations are removed. **Of note, the variabilities indicated in Figure 2 quantify instabilities of internal optics only. They do not track changes in responsivity resulting from the punctured diffuser.**

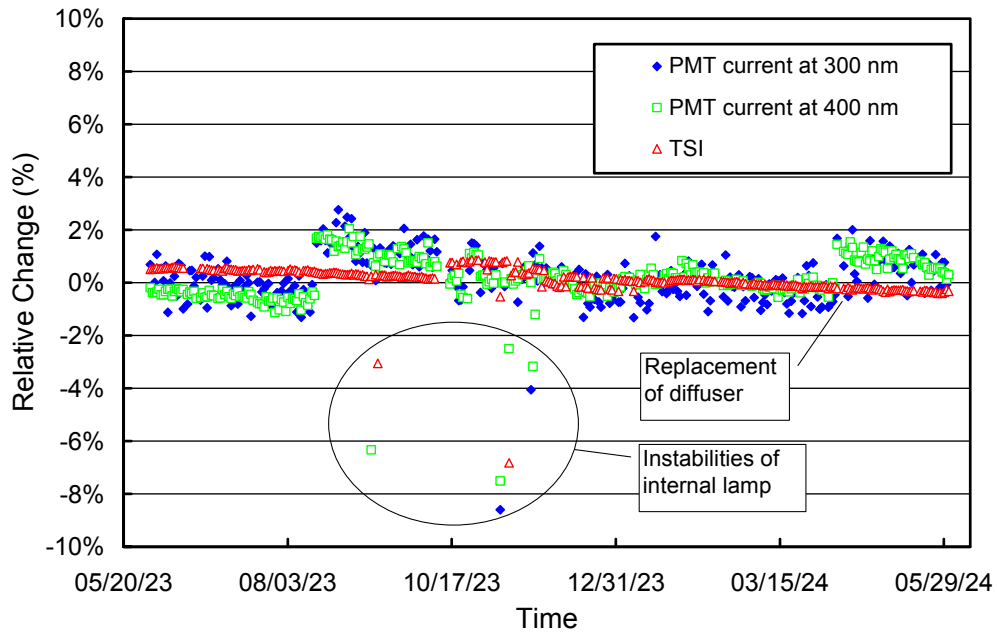


Figure 2. Time-series of PMT current at 300 and 400 nm, and TSI signal. All data were extracted from measurements of the internal irradiance standard and are normalized to their average.

The reporting period was divided into 20 calibration periods due to the large variations in responsivity resulting from the punctured diffuser. An overview of these periods is provided in Table 1. Note that calibrations P4 and P6 were used in more than one period. Figure 3 shows ratios of the calibration functions applied during Periods P1 through P16 relative to the function of Period P1.

Table 1. Calibration periods for Palmer Volumes 33.

| Calibration identifier | Period range | Number of absolute scans | Remarks |
|------------------------|---------------------|--------------------------|----------------------|
| P1 | 06/01/23 – 07/07/23 | 3 | Standard calibration |
| P2 | 07/08/23 – 08/21/23 | 3 | Standard calibration |
| P3 | 08/22/23 – 09/08/23 | 2 | Standard calibration |
| P4 | 09/09/23 – 09/13/23 | 3 | Standard calibration |
| P4 4 | 09/14/23 – 09/18/23 | 0 | P4, scaled by 1.04 |
| P4 | 09/19/23 – 09/19/23 | 3 | Standard calibration |
| P4 8 | 09/20/23 – 09/20/23 | 1 | P4, scaled by 1.08 |
| P4 55 | 09/21/23 – 09/21/23 | 0 | P4, scaled by 1.055 |
| P4 | 09/22/23 – 10/05/23 | 3 | Standard calibration |
| P4 8 | 10/06/23 – 10/08/23 | 0 | P4, scaled by 1.08 |
| P4 | 10/09/23 – 10/20/23 | 3 | Standard calibration |
| P6 | 10/21/23 – 10/28/23 | 6 | Standard calibration |
| P6 7 | 10/29/23 – 10/29/23 | 1 | P6, scaled by 1.07 |
| P6 | 10/30/23 – 11/17/23 | 6 | Standard calibration |
| P6 6 | 11/18/23 – 11/18/23 | 0 | P6, scaled by 1.06 |
| P6 8 | 11/19/23 – 11/19/23 | 0 | P6, scaled by 1.08 |
| P6 | 11/20/23 – 03/11/24 | 6 | Standard calibration |
| P6A | 03/12/24 – 03/31/24 | 0 | P6, scaled by 0.96 |
| P6 | 04/01/24 – 04/08/24 | 6 | Standard calibration |
| P9 | 04/09/24 – 05/31/24 | 3 | Standard calibration |

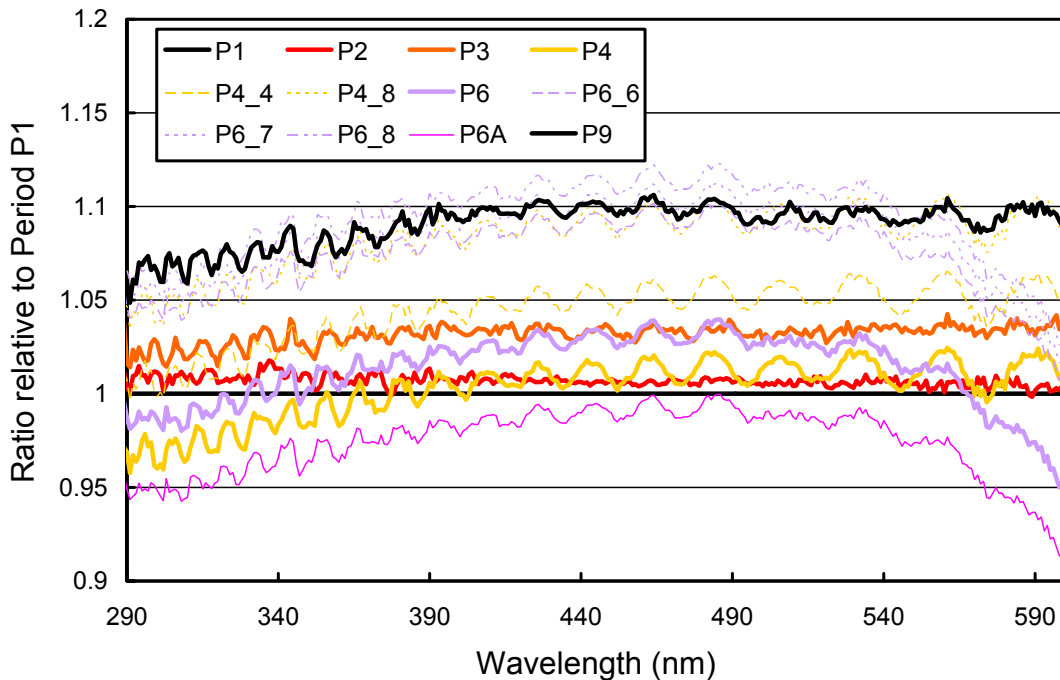


Figure 3. Ratios of spectral irradiance assigned to the internal reference lamp for periods P1 – P9, relative to Period P1. Functions that were established using standard calibration methods are printed in bold. Functions that were derived by scaling with GUV-511 data are indicated by thin lines.

Figure 4 shows the ratio of GUV-511 data (340 nm channel) and final SUV-100 measurements, which were weighted with the spectral response function of this channel. The ratio is normalized and should ideally be one. With the exception of a few outliers, GUV-511 and SUV-100 measurements agree to within $\pm 10\%$. The standard deviation is 0.024. (For comparison, the standard deviation of similar data of the 2021/22 (Volume 31) period, which was not affected by a punctured diffuser, was also 0.024, indicating that the uncertainty of SUV-100 data of the current period that were included in the published dataset is similar to that of the 2021/22 period.)

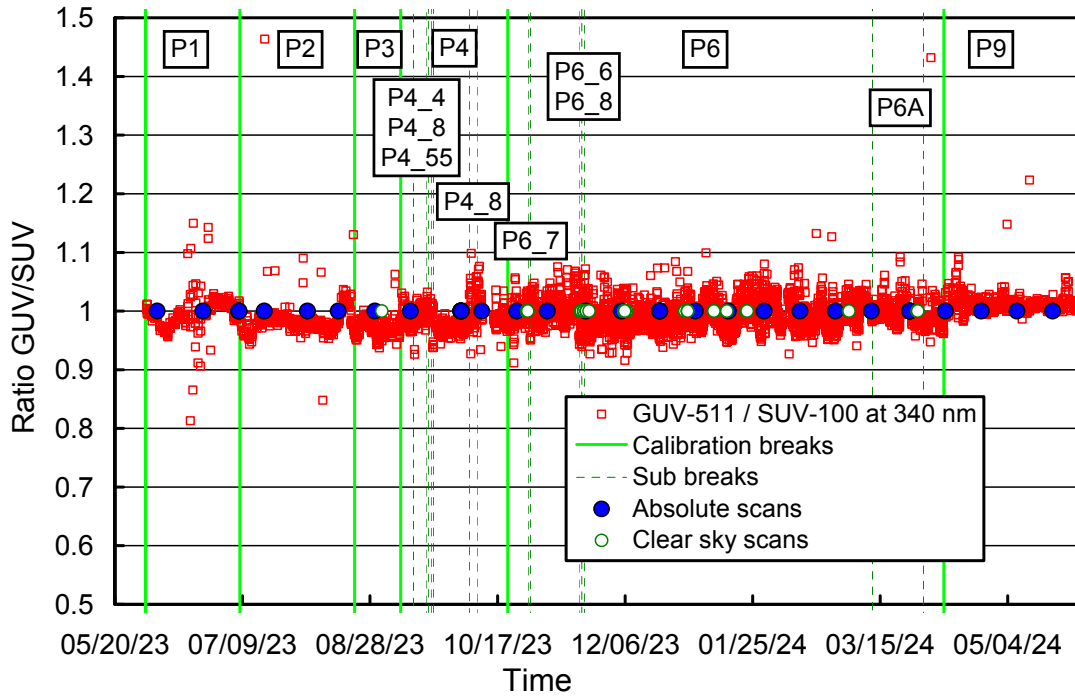


Figure 4. Ratio of GUV-511 measurements at 340 nm with SUV-100 measurements. The latter were weighted with the spectral response function of the GUV-511’s 340 nm channel. Labels indicate calibration periods defined in Table 1.

2.3. Wavelength Calibration

Wavelength stability of the system was monitored with the internal mercury lamp. Information from the daily wavelength scans was used to homogenize the data set by correcting day-to-day fluctuations in the wavelength offset. The wavelength-dependent bias of this homogenized dataset and the correct wavelength scale was determined with the Version 2 Fraunhofer-line correlation method (Bernhard et al., 2004). Figure 5 shows the correction function calculated with this algorithm. Figure 6 indicates the wavelength accuracy of Version 0 data for five wavelengths in the UV and visible range, obtained by running the Fraunhofer-line correlation method for a second time. Shifts are typically smaller than ± 0.1 nm. (The standard deviations for wavelengths between 305 and 400 nm are 0.032 nm on average). There are several steps in this time series for various reasons. The wavelength accuracy was further improved as part of the production of Version 2 data. Figure 7 shows the wavelength accuracy of Version 2 data. There are no step-changes and the standard deviations for wavelengths between 305 and 400 nm decreased to 0.022 nm.

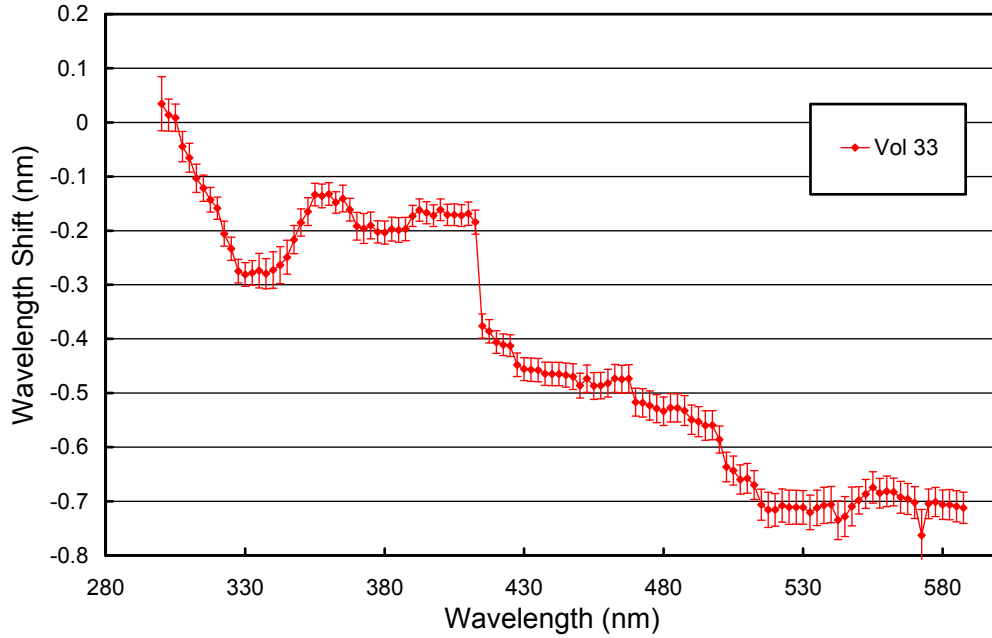


Figure 5. Monochromator mapping function. Error bars indicate 1- σ variation.

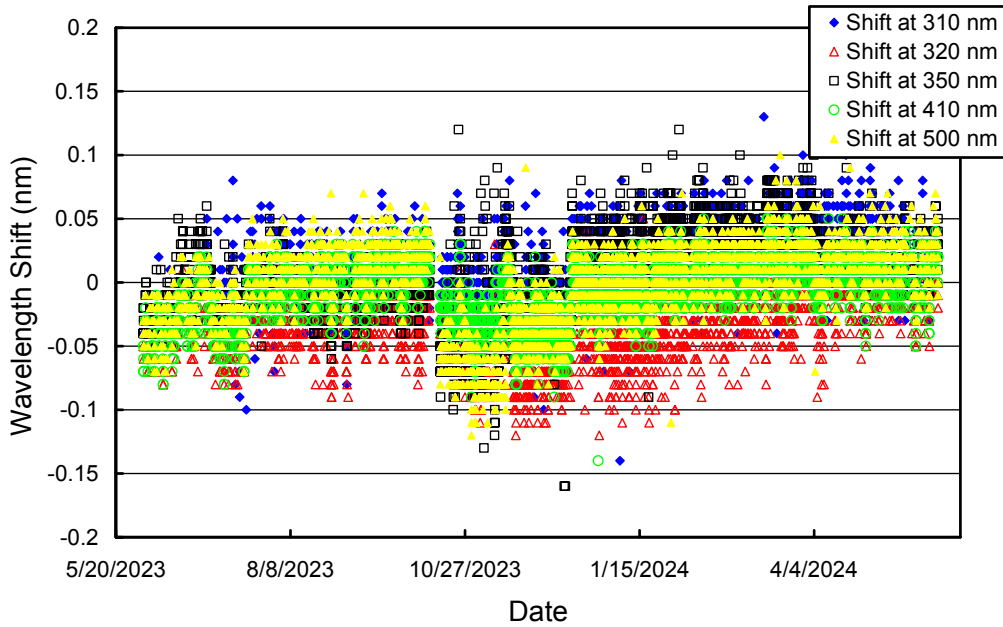


Figure 6. Wavelength accuracy check of *Version 0* data at five wavelengths by means of Fraunhofer-line correlation. Measurements were evaluated in hourly increments.

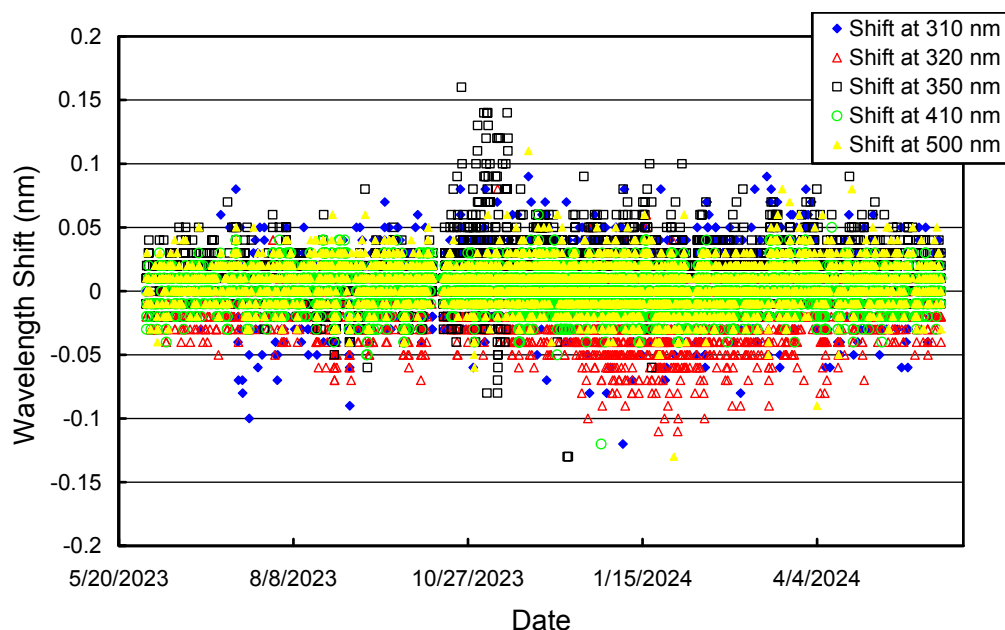


Figure 7. Same as Figure 6 but for Version 2 data.

2.4. Missing data

Table 2 provides a list of missing days in the published dataset. The letters A, M, N, and D after each date indicate whether afternoon, morning, or noon data, or data of the whole day are missing, respectively. Many data gaps are caused by instabilities in the instrument’s responsivity caused by the punctured diffuser, which could not be corrected.

Table 2. Days with substantial data gaps.

| Date | Date | Date | Date | Date | Date | Date |
|-------------|---------------|--------------|----------------|--------------|---------------|---------------|
| 7/7/23 (M) | 9/5/23 (M) | 10/13/23 (D) | 10/25/23 (M,N) | 1/20/24 (M) | 2/28/24 (D) | 4/9/24 (M) |
| 7/28/23 (N) | 9/21/23 (A) | 10/14/23 (D) | 11/14/23 (M) | 2/5/24 (N,A) | 2/29/24 (M,N) | 4/11/24 (D) |
| 8/16/23 (M) | 9/22/23 (M) | 10/15/23 (D) | 11/15/23 (A) | 2/6/24 (D) | 3/8/24 (M,N) | 4/15/24 (A) |
| 8/23/23 (A) | 10/1/23 (M,N) | 10/17/23 (M) | 11/17/23 (M) | 2/7/24 (M,N) | 3/10/24 (D) | 4/23/24 (M) |
| 8/31/23 (A) | 10/2/23 (N) | 10/20/23 (A) | 12/16/23 (M) | 2/15/24 (D) | 3/11/24 (M) | 5/16/24 (D) |
| 9/3/23 (D) | 10/11/23 (D) | 10/21/23 (M) | 1/12/24 (M) | 2/19/24 (A) | 3/26/24 (M) | 5/17/24 (M,N) |
| 9/4/23 (D) | 10/12/23 (D) | 10/22/23 (A) | 1/19/24 (D) | 2/20/24 (M) | 4/3/24 (M) | 5/18/24 (M,N) |

References

Bernhard, G., C. R. Booth, and J. C. Ehamjian. (2004). Version 2 data of the National Science Foundation’s Ultraviolet Radiation Monitoring Network: South Pole, *J. Geophys. Res.*, 109, D21207, doi:10.1029/2004JD004937.

Bernhard G. and S. Stierle (2020). Trends of UV Radiation in Antarctica, *Atmosphere*, 11(8), 795, doi: https://doi.org/10.3390/atmos11080795.